

# Artificial nerve graft constructed by coculture of activated Schwann cells and human hair keratin for repair of peripheral nerve defects

Han-Jun Qin<sup>1, #</sup>, Hang Li<sup>2, #</sup>, Jun-Ze Chen<sup>3</sup>, Kai-Rui Zhang<sup>1</sup>, Xing-Qi Zhao<sup>1</sup>, Jian-Qiang Qin<sup>4</sup>, Bin Yu<sup>1, \*,</sup>, Jun Yang<sup>1, 5, \*</sup>

<https://doi.org/10.4103/1673-5374.355817>

Date of submission: March 11, 2022

Date of decision: June 6, 2022

Date of acceptance: August 16, 2022

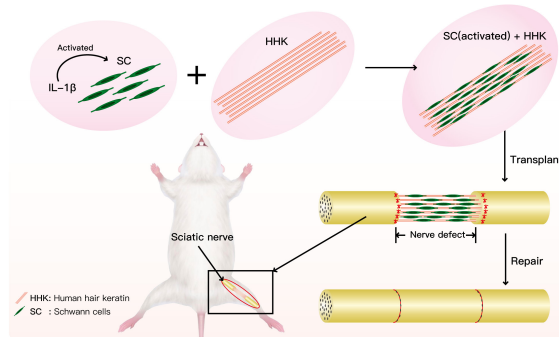
Date of web publication: October 10, 2022

## From the Contents

Introduction	1118
Methods	1119
Results	1120
Discussion	1121

## Graphical Abstract

Artificial nerve loaded with Schwann cells and human hair keratin to bridge peripheral nerve defects



## Abstract

Studies have shown that human hair keratin (HHK) has no antigenicity and excellent mechanical properties. Schwann cells, as unique glial cells in the peripheral nervous system, can be induced by interleukin-1 $\beta$  to secrete nerve growth factor, which promotes neural regeneration. Therefore, HHK with Schwann cells may be a more effective approach to repair nerve defects than HHK without Schwann cells. In this study, we established an artificial nerve graft by loading an HHK skeleton with activated Schwann cells. We found that the longitudinal HHK microfilament structure provided adhesion medium, space and direction for Schwann cells, and promoted Schwann cell growth and nerve fiber regeneration. In addition, interleukin-1 $\beta$  not only activates Schwann cells, but also strengthens their activity and increases the expression of nerve growth factors. Activated Schwann cells activate macrophages, and activated macrophages secrete interleukin-1 $\beta$ , which maintains the activity of Schwann cells. Thus, a beneficial cycle forms and promotes nerve repair. Furthermore, our studies have found that the newly constructed artificial nerve graft promotes the improvements in nerve conduction function and motor function in rats with sciatic nerve injury, and increases the expression of nerve injury repair factors fibroblast growth factor 2 and human transforming growth factor B receptor 2. These findings suggest that this artificial nerve graft effectively repairs peripheral nerve injury.

**Key Words:** artificial nerve graft; bioactive; human hair keratin; interleukin-1 $\beta$ ; macrophages; nerve graft; nerve growth factor; nerve repair; peripheral nervous injury; Schwann cells

## Introduction

Surgical techniques for transection injury to the peripheral nerve vary based on the injury severity, though primary end-to-end nerve repair is the preferred treatment. If the primary repair is not possible because of severe local tissue trauma or retraction of the distal or proximal nerve stump, a graft can be inserted between the two nerve ends to achieve tension-free repair (Campbell, 2008). Autogenous nerve grafts, most commonly taken from the sural nerve, have long been considered the gold standard for peripheral nerve repair, but they are technically challenging because of the sophisticated microsurgical skills required and donor site morbidity (Schultz et al., 1992). Alternatives to autografts are currently being investigated in preclinical studies and clinical trials.

Unlike the central nervous system, the peripheral nervous system shows remarkable regenerative abilities after injury (Gu et al., 2014; Li et al., 2021; Hu et al., 2022). However, peripheral nervous system regeneration is often incomplete and defects at nerve endings are common (Benowitz and Popovich, 2011). The development of neural tissue engineering provides a

possibility to repair injured peripheral nerves (Knowlton et al., 2018). The ideal characteristics of artificial nerves are as follows: no antigenicity and can show normal action potential conduction. Axons of artificial nerves can accurately reach target tissues or organs through graft regeneration so that nerves and organs can quickly obtain blood supply to achieve a certain degree of regeneration (Gu et al., 2011; Chiono and Tonda-Turo, 2015).

A hair follicle is a structure that is selectively degraded and regenerated in the human body. In recent years, hair follicles have become a focus of regenerative biological materials research (Sierpinski et al., 2008; Hwang et al., 2013; Pace et al., 2013; Kiani et al., 2018). Keratin, a major component of hair (Shavandi et al., 2017), exists in the form of microfilaments and a matrix. Keratin predominantly contains more than 20 types of amino acids, including cystine, glycine and lysine. Trace elements, such as copper, zinc, manganese and melanin, can also be found. The chemical structure of keratin is divided into three types according to the intermolecular interaction forces: hydrogen bonds, salt bonds, and two sulfur bonds (de Guzman et al., 2011). Keratin has been used successfully in a previous study to repair peripheral nerve injury (Pace et al., 2013), but how cells work together with keratin to repair

<sup>1</sup>Department of Orthopedics, Nanfang Hospital, Southern Medical University; Guangdong Provincial Key Laboratory of Bone and Cartilage Regenerative Medicine, Nanfang Hospital, Southern Medical University, Guangzhou, Guangdong Province, China; <sup>2</sup>Hebei Medical University, Shijiazhuang, Hebei Province, China; <sup>3</sup>Department of Orthopedics, Baiyun Branch of Southern Hospital, Guangzhou, Guangdong Province, China; <sup>4</sup>Department of Anatomy, School of Basic Medical Sciences, Southern Medical University, Guangzhou, Guangdong Province, China; <sup>5</sup>Department of Orthopedics, The 74<sup>th</sup> Group Military Hospital of PLA, Guangzhou, Guangdong Province, China

\*Correspondence to: Jun Yang, PhD, yangjun201911@sina.com; Bin Yu, PhD, yubin@smu.edu.cn.

<https://orcid.org/0000-0002-9982-6157> (Han-Jun Qin)

#Both authors contributed equally to this work.

**Funding:** The study was supported by Military Medical Science & Technology Youth Training Program, No. 19QN005; and President Foundation of Nanfang Hospital, Southern Medical University, No. 2020B028 (both to JY).

**How to cite this article:** Qin HJ, Li H, Chen JZ, Zhang KR, Zhao XQ, Qin JQ, Yu B, Yang J (2023) Artificial nerve graft constructed by coculture of activated Schwann cells and human hair keratin for repair of peripheral nerve defects. *Neural Regen Res* 18(5):1118-1123.

peripheral nerve damage has not been explored.

Schwann cells, as unique glial cells of the peripheral nervous system, play an important role in peripheral nerve generation, development, and morphological and functional maintenance (Jessen and Mirsky, 2016; Clements et al., 2017). After peripheral nerve injury, four main cell types are involved in the regeneration process of peripheral nerves, which are Schwann cells, macrophages, fibroblasts, and vascular endothelial cells (Cattin and Lloyd, 2016). Of these cell types, Schwann cells and macrophages are most important. Macrophages, and their related cytokine induction and regulation, stimulate proliferation of Schwann cells and secretion of nerve growth factors (NGFs). Schwann cells secrete cytokines that inhibit macrophage migration, and promote the secretion and expression of active substances of macrophages such as interleukin-1. This further promotes Schwann cell proliferation and axon regeneration, both of which promote nerve regeneration and repair (Cattin et al., 2015; Chen et al., 2015; Kessler et al., 2018). High interleukin-1 $\beta$  (IL-1 $\beta$ ) expression may help fibroblasts to secrete granulocyte-macrophage colony-stimulating factor and induce Schwann cells to secrete NGF and promote nerve regeneration (Chen et al., 2015).

In this study, we constructed artificial nerves with IL-1 $\beta$ -activated Schwann cells and human hair keratin (HHK) *in vitro*. *In vitro* and *in vivo* experiments were conducted to evaluate the expression of important nerve factors and their role in promoting neural repair under the condition of cell-scaffold material interaction during artificial neural construction. Our study aimed to clarify whether new artificial nerves can be used as potential grafts for nerve transection injuries and to provide a therapeutic perspective for the clinical application of the artificial nerves for peripheral nerve injury repair.

## Methods

### Primary culture and identification of Schwann cells

All experiments were approved by the Institutional Animal Care and Use Committee of Southern Medical University (Guangzhou, China; approval No. NFYY-2021-61) on March 18, 2021. All animal experiments were designed and reported according to the Animal Research: Reporting of *In Vivo* Experiments (ARRIVE) guidelines (Kilkenny et al., 2010). All Sprague Dawley rats (specific pathogen-free level) were provided by the Animal Center of Southern Medical University (license No. SCXK (Yue) 2021-0041). All rats were anesthetized by abdominal injection (3% pentobarbital sodium, 40 mg/kg) and then cervically dislocated.

Bilateral sciatic nerves and brachial plexus in two 4- or 5-day-old Sprague-Dawley rats were removed under sterile conditions. The epineurium was dissected under a dissecting microscope (Ningbo Cheng-He Microsurgical Instruments Factory, Ningbo, China) and placed in Dulbecco's modified Eagle medium: nutrient mixture F-12 (DMEM/F12) (Gibco, Gaithersburg, CA, USA). Nerve bundles were cut into 0.1–0.2 mm<sup>3</sup> fragments in DMEM/F12 medium. Then, 0.16% collagenase (Gibco) and 0.25% trypsin (Thermo Fisher, Rockford, MA, USA) were added to the fragments, mixed thoroughly at 37°C, and placed in a 5% CO<sub>2</sub> incubator for 5 minutes. To stop digestion, DMEM/F12 medium containing 10% fetal bovine serum was added for 5–10 minutes. Next, the suspension was placed in a centrifuge tube and the precipitated portion was further digested with 1 mL 0.16% collagenase. At the end of digestion, 2–3 mL of D-Hank's solution (Pythnbio, Guangzhou, China) was added to the suspension. Once most of the undigested tissue was precipitated, the suspension was added to a centrifuge tube and centrifuged at 200 × *g* for 10 minutes. To further purify Schwann cells, we digested them again with trypsin on the 5<sup>th</sup> day of culture. Because of the weak adhesion of Schwann cells, during digestion, if Schwann cells shrunk back under the electron microscope, digestion would be stopped immediately, and the digested Schwann cells would be gently blown down and centrifuged for subculture. Subsequently, partially purified Schwann cells were selected for staining verification. Schwann cells were stained using an S100 protein SABC Kit (Boster Biological Technology, Wuhan, China), plated onto slides at a density of 1 × 10<sup>5</sup> cells/mL and fixed in 4% paraformaldehyde. Blood-derived peroxidase was blocked with 1% hydrogen peroxide. Next, the Schwann cells were further selected from fibroblasts using mouse anti-S100 antibody (monoclonal, Boster Biological Technology, Cat# BMO120, RRID: AB\_2716291). Briefly, the Schwann cells were incubated with anti-S100 primary antibody at 4°C overnight, and then with the secondary antibody, biotinylated goat anti-mouse IgG (Abcam, Cambridge, MA, USA, Cat# ab6788, RRID: AB\_954885, 1:500), at 37°C for 1 hour. SABC was added at 37°C for 20 minutes before 3,3'-diaminobenzidine color chips were added (Tao, 2013).

### Preparation of nerve homogenate

The skin over the posterior femur was aseptically incised in the same Sprague Dawley rats as were used above. Muscles were isolated to expose the sciatic nerve, which was cut in the proximal ischial foramen (pre-ulcer for 24 hours). Twenty-four hours later, the incision suture was removed to re-expose the sciatic nerve, which was approximately 1 cm long and completely disconnected from the suture site. The nerves were dissected under an inverted microscope (CXK4, Olympus, Tokyo, Japan) and mixed in 15 mL of DMEM/F12 medium to produce nerve tissue homogenate suspension for activation of macrophages.

### EdU assay

Proliferation of Schwann cells cultured in differently conditioned media was detected in a 5-ethynyl-2'-deoxyuridine (EdU) incorporation assay, using the YF@555 Click-iT EdU Imaging Kits (C6016M, UELandy, Suzhou, China).

Schwann cells were cultured in normal medium (group A), macrophage-conditioned medium (group B), activated macrophage medium (group C) or IL-1 $\beta$  medium (group D). Medium composition of the four groups were: group A, purified Schwann cells in 10% fetal bovine serum-DMEM/F12 medium; group B, Schwann cells in macrophage-conditioned medium, where macrophages were extracted according to a previous report (Liu et al., 2021); group C, Schwann cells in conditioned medium of macrophages activated by nerve homogenate (nerve homogenates were injected back into the abdominal cavity of rats and peritoneal macrophages were collected 3 days later to obtain activated macrophages); group D, Schwann cells in 10% fetal bovine serum-DMEM/F12 medium containing IL-1 $\beta$  (2.0 ng/mL; Peprotech, Rocky Hill, NJ, USA). After the cells were cultured in different media for 24 and 48 hours, an EdU experiment was performed to detect cell proliferation. EdU reagent (10  $\mu$ M) was added to each well and incubated for 2 hours at room temperature, then the Click-it reaction mixture was added for reaction, and nuclei were stained with Hoechst 33342. A fluorescence microscope (IX73, Olympus) was used for photography. At high magnification, three random fields of each well were selected, and the average number of positive cells was calculated.

The same method was used to detect the proliferation of macrophages cultured in the different conditioned media. The four groups were: group E, 10% fetal bovine serum-DMEM/F12 medium for normal macrophage culture; group F, macrophages activated by nerve homogenate; group G, Schwann cell-conditioned medium; and group H, conditioned medium of Schwann cells activated by 2.0 ng/mL IL-1 $\beta$ .

### Enzyme-linked immunosorbent assay

Enzyme-linked immunosorbent assay (ELISA) was used to detect NGF levels in Schwann cells cultured in different conditioned media. Purified Schwann cells were cultured at 37°C in 5% CO<sub>2</sub> for 3 days, and then centrifuged at 300 × *g* for 10 minutes to obtain the supernatant. NGF level in the supernatant was detected by an NGF ELISA kit (DY556, R&D, Biotechne, UK), with absorbance at 450 nm measured by a microplate reader (SpectraMax M4, Molecular Devices, Sunnyvale, CA, USA). NGF levels in the supernatants were calculated according to a standard curve.

The same method was used to detect IL-1 $\beta$  levels in macrophages cultured in different conditioned media. Macrophages were cultured at 37°C and 5% CO<sub>2</sub>. Macrophage culture supernatants were collected and IL-1 $\beta$  level was detected using an IL-1 $\beta$  ELISA kit (RLB00, R&D). Absorbance was measured using an enzyme labeling instrument (SpectraMax M4, Molecular Devices). IL-1 $\beta$  expression in the supernatants was calculated from the standard curve.

### Activated Schwann cells combined with HHK for artificial nerve construction

The HHK scaffold was provided by the Department of Anatomy, Southern Medical University (Xu et al., 2003). The HHK catheter supplied had an inner diameter of 2.1 mm, a wall thickness of 1.8 mm and a length of 12 mm. HHK powder was then prepared. Human hair fiber pieces were added to 0.1 M NaOH solution at a ratio of 1:15 and stirred. Heat treatment was performed in a water bath for 1 hour at 80°C. Fibers were filtered using 300 nylon filters (Sigma-Aldrich, St Louis, MO, USA) and washed repeatedly with distilled water to approximately pH 7.0. Human hair fiber debris was added at a ratio of 1:15 to a reducing system containing sodium sulfite, urea, and sodium alkylsulfonate. Dialysate solution was poured into a beaker and dried in a vacuum oven to produce light brown keratin powder. Schwann cells were activated with 2.0 ng/mL IL-1 $\beta$  for 72 hours and prepared into a 1 × 10<sup>7</sup>/mL cell suspension for later use. HHK catheters were coated with 30% extracellular matrix (ECM) gel (Thermo Fisher) and soaked in activated Schwann cell suspension after natural drying. HHK powder was added into the cell suspension (0.1 mg/mL), cocultured for 6 hours, removed and placed in a 24-well plate before soak culture was continued for 48 hours. They were then removed and further modified with 30% ECM gel to obtain prefabricated HHK artificial nerve-bridge grafts. The HHK scaffold during its preparation and electron microscopy of the artificial nerve after successful construction (after coculture with IL-1 $\beta$ -activated Schwann cells) is shown in **Additional Figure 1A** and **B**.

### Animal models and surgery

Two-month-old Sprague-Dawley male rats (specific pathogen-free level, body weight 220–250 g) were given normal diet and normal activity in a standard environment. All animals were housed in the Animal Facility of the Nanfang hospital, with a 12-hour light/dark cycle, 25°C room temperature and 50% relative humidity, and three rats in each cage. Rats were randomly divided into two groups (*n* = 6). All rats were anesthetized by abdominal injection of 3% pentobarbital sodium (40 mg/kg; Sigma, St Louis, MO, USA). For the direct suture group (control group), the sciatic nerve was exposed under aseptic conditions and a 3-cm nerve segment was dissociated. A 1-cm middle nerve segment was excised and the defect was directly sutured. For the HHK group, the sciatic nerve was also exposed under sterile conditions and a 1-cm middle nerve segment was excised. The prefabricated HHK artificial nerve-bridge (10 mm) was then anastomosed to the broken nerve ends under a microsurgical microscope (Cheng-He Microsurgical Instruments Factory, Ningbo, China). All procedures were performed under a microscope by an experienced surgeon. To avoid possible operative errors, all of the modeling was done by the same surgeon.

### In situ hybridization

*In situ* hybridization detection was performed to determine HHK degradation

and NGF expression in the sciatic nerve using frozen sections and an NGF probe. The sciatic nerve, which was used for artificial nerve transplantation to repair sciatic nerve defects, was removed from rats under sterile conditions after anesthesia by abdominal injection (3% pentobarbital sodium, 40 mg/kg). After the nerve was quickly placed into liquid nitrogen, tissue sections were prepared. The sections were fixed with 4% paraformaldehyde, fully washed with ddH<sub>2</sub>O, digested with pepsin, and fully washed again with ddH<sub>2</sub>O. They were then fixed with 1% paraformaldehyde and incubated at 40°C for 3–5 hours after addition of prehybrid liquid. Digoxin-labeled oligonucleotide probe hybrids (Gefan Biotechnology Company, Shanghai, China) were added after denaturation (5'-GCC TGG CTT CTT GGG TTC ACC GCA T-3') and incubated overnight at 40°C. After posthybrid washing, blocking solution and biotinylated anti-rat digoxin were added, and sections were washed in 0.5 M phosphate-buffered saline. Then, biotinylated peroxidase was added, followed by washing in 0.5 M phosphate-buffered saline and 3,3'-diaminobenzidine coloring. After conventional hematoxylin nuclear staining, sections were mounted. Positive cells were observed under the fluorescence microscope (BX63, Olympus).

#### Electrophysiological detection

Electrophysiology was used to assess peripheral nerve function. Anesthetized rats were placed in a stereotaxic frame to expose their bilateral lower extremities. A concentric round needle was inserted into the gastrocnemius muscle as the recording electrode, with a saddle electrode (Nicolet VikingQuest, WI, USA) used as a stimulus electrode for placement of the proximal sciatic nerve (the surgical side was placed beside the heart). The cathode was placed at the distal end of the stimulus and the anode at the proximal end. An electromyography and evoked potential apparatus (Nicolet VikingQuest) was used for the tibiofibular motor conduction interface. The scanning speed was 2 ms; sensitivity, 5 mV; duration of stimulation, 0.1 ms; stimulation frequency, 1 Hz; and stimulation intensity, 14–20 mA. Left and right sciatic nerves were repeatedly stimulated. Recordings were made for values of latency negative phase wave amplitude and time limit of compound muscle action potentials at 2, 4, 6 and 8 weeks after artificial nerve transplantation.

#### Gait analysis

Peripheral nerve repair was evaluated by gait analysis. A dark box was prepared before gait analysis. The rat was placed at the entrance of the dark box and was allowed to walk independently throughout the box so that its red footprints were left on the white paper. The footprints were recorded after operation at 2, 4, 6 and 8 weeks. The experiment was repeated three times for each rat, and the average value was used for statistical analysis.

Recordings were made for indicators of footprint on the experimental side (E); normal footprint (N); print length (PL), distance from heel to toe; total spreading (TS), distance between the first toe and the fifth toe; and intermediate toes (IT), distance between the second and the fourth toes. Sciatic function index (SFI) was calculated using the following formula.  $SFI = -38.3 \times [PL(E) - PL(N)] / PL(N) + 109.5 \times [TS(E) - TS(N)] / TS(N) + 13.3 (2) \times [IT(E) - IT(N)] / IT(N) - 8.8$  (Rao et al., 2020). An SFI of 0 indicates completely normal nerve function, -100% indicates complete loss of nerve function, and 0–100% indicates partial recovery of nerve function.

#### Immunohistochemical staining

Immunohistochemical staining was used to evaluate related nerve repair factors. At week 8 after the operation, the rats were euthanized by abdominal injection of 3% pentobarbital sodium (40 mg/kg) and the sciatic nerve was quickly removed and fixed in paraformaldehyde for 24 hours. The specimens were dissected within 5 mm of the suture end for dehydrated paraffin embedding, and the thickness of each specimen was 4 μm for section staining. The specimens were treated for antigen repair by boiling in an ethylenediaminetetraacetic acid repair solution (pH 9.0) for 2 minutes and were then cooled to room temperature. For immunohistochemical staining, primary antibodies S100 (Abclonal, Wuhan, China, Cat# A19108, RRID: AB\_2862601, rabbit, mAb, 1:100), vascular endothelial growth factor (VEGF; Abclonal, Cat# A12303, RRID: AB\_2759160, rabbit, mAb, 1:100), transforming growth factor beta receptor type II (TGFBR2; Abclonal, Cat# A1415, RRID: AB\_2761007, rabbit, mAb, 1:50), fibroblast growth factor-2 (FGF2; Abclonal, Cat# A0235, RRID: AB\_2757048, rabbit, mAb, 1:50) and platelet-derived growth factor receptor beta (PDGFR-β; Abclonal, Cat# A2180, RRID: AB\_2764198, rabbit, mAb, 1:100) were incubated overnight at 4°C. Horseradish peroxidase-conjugated anti-rabbit IgG (ready to use, ZSGB-BIO, Beijing, China, Cat# PV-6001, RRID: AB\_2864333) was used as a secondary antibody. Specimens were incubated in the secondary antibody at 37°C for 1 hour. Horseradish peroxidase-streptavidin detection system (Maxim, Fuzhou, China, Cat# DAB4033) was used to detect immunoreactivity and hematoxylin was used for counterstaining. Immunofluorescent staining was performed using a standard protocol. After the specimens were dewaxed, the sections were placed into 3% H<sub>2</sub>O<sub>2</sub> for blocking, and then 10% goat serum was added to block at room temperature for 30 minutes. Finally, sections were incubated with primary antibodies S100 antibody (Abclonal, Cat# A19108, RRID: AB\_2862601, rabbit, mAb, 1:100) and proliferating cell nuclear antigen (PCNA) antibody (Affinity Biosciences, Beijing, China, Cat# DF6067, RRID: AB\_2838035, rabbit, pAb, 1:100) at 4°C overnight. Secondary antibody (goat anti-rabbit IgG, Dylight 488, Abbkine, Wuhan, China, Cat# A23220, RRID: AB\_2737289, 1:200; goat anti-rabbit IgG (H+L) Fluor594-conjugated,

Affinity Biosciences, Cat# S0006, RRID: AB\_2843436, 1:200) conjugated with fluorescence was added to the sample sections, and incubated for 1 hour at room temperature. Finally, 4',6-diamidino-2-phenylindole (Solarbio, Beijing, China, Cat# S2110) was added to the specimens and the slices were sealed. A fluorescence microscope was used to detect the expression of S100 (green) and PCNA (red) with excitation wavelength 488 and 594, respectively. The number of positive cells observed at high magnification (200×) was calculated in three random fields.

#### Statistical analysis

No statistical methods were used to predetermine sample sizes; however, our sample sizes were similar to those reported in a previous publication (Wang et al., 2017). No animals or data points were excluded from the analysis. The investigators were blind to allocation during experiments and outcome assessment. SPSS software (version 19.0; IBM Corp., Armonk, NY, USA) was used for all statistical analyses. Shapiro-Wilk test was used to test the normality of the data. When data were normally distributed and had homogeneity of variance, all graphical data were presented as mean ± standard deviation. One-way analysis of variance was used for three or more groups. The Student-Newman-Keuls *post hoc* tests were used for further multiple comparisons. Independent sample *t*-tests were performed for comparison of two groups. The level of significance was set at  $P < 0.05$ .

## Results

### Cell proliferation and NGF and IL-1β secretion in different conditioned media

According to the EdU results at 24 and 48 hours, groups C and D had stronger Schwann cell proliferation ability than groups A and B, and group D had the strongest proliferation ability. These results suggest that 2.0 ng/mL IL-1β promoted Schwann cell proliferation (Figure 1A). In the proliferation activity test of macrophages, the strongest macrophage proliferative activity was in group H. Conditioned medium of Schwann cells activated by 2.0 ng/mL IL-1β promoted macrophage proliferation (Figure 1B). ELISA was used to detect NGF levels in the different groups, and showed that of the four groups, group D had the highest NGF level in Schwann cells (Figure 1C). IL-1β levels in groups F and H were significantly higher than those in groups E and G. Conditioned medium of macrophages activated by nerve homogenate and conditioned medium of Schwann cells activated by 2.0 ng/mL IL-1β both led to high IL-1β expression in macrophages (Figure 1D).

### The bioactive artificial nerve improves nerve conduction capacity after sciatic nerve injury

Latency, time limit and amplitude were recorded at 2, 4, 6 and 8 weeks after artificial nerve transplantation. Latency, which reflects the time of rapid conduction fibers in nerve axons reaching muscles (Valentino et al., 2007), was lengthened and conduction velocity was slowed after nerve injury (Figure 2A). Time limit showed the discharge of each single muscle fiber at the same time. After nerve injury, the time limit was prolonged and the waveform was discrete (Figure 2B). Amplitude, which reflects the number of muscle fibers involved in mixed muscle action potentials (Valentino et al., 2007), was reduced after nerve injury (Figure 2C). At 8 weeks after surgery, each of the electrophysiological parameters were improved compared with those at 2 weeks after surgery, suggesting that the damaged nerve tissue was in a state of functional repair. The latency in the HHK group was significantly lower than that of the control group at all time points, indicating that the time for the HHK group axon fast conduction fiber to reach muscle was shorter. The time limit data showed that the muscle discharge duration extension was shorter after nerve injury in the HHK group compared with that in the control group. The results of the amplitude reflected that the number of muscle fibers involved in the mixed muscle action potential in the HHK group was more than that in the control group. These results indicate that the use of newly constructed artificial nerves may lead to a significantly better nerve repair result than direct suturing.

### The bioactive artificial nerve improves sciatic function after sciatic nerve injury

According to SFI data, nerve function in the two groups was completely lost at 2 weeks, but the nerve in the HHK group showed obvious repair after 6 weeks. At week 8, the sciatic nerve function was significantly improved in the HHK group compared with that in the control group, which suggested significantly faster nerve repair in the HHK group (Figure 3A and B).

### The bioactive artificial nerve promotes Schwann cell proliferation in the injured area after sciatic nerve injury

Immunohistochemical staining showed that the number of S100-positive cells was significantly greater in the HHK group than in the control group (Figure 4A). Immunofluorescence also showed that the number of PCNA-positive cells was higher in the HHK group than in the control group (Figure 4B). The results indicated that the artificial nerve significantly promoted Schwann cell proliferation.

### The bioactive artificial nerve promotes NGF secretion in sciatic nerve

In situ hybridization was used to detect the expression of NGF, an important factor in nerve repair. NGF expression in the HHK group was much higher than that in the control group, suggesting that the artificial nerve promoted NGF secretion and thus accelerated nerve repair (Figure 5).

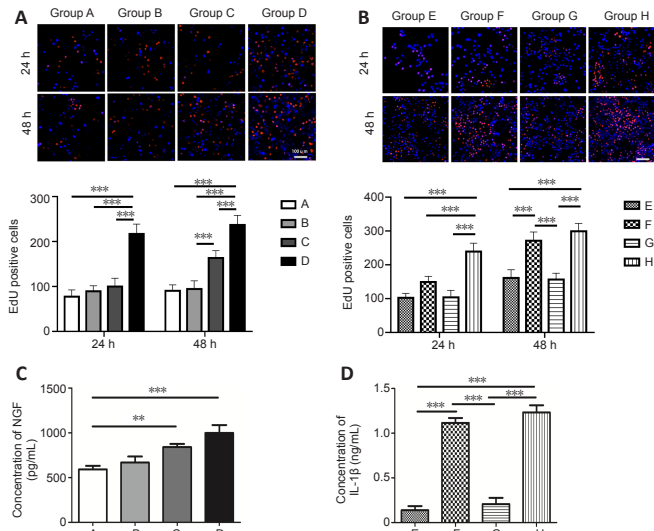


**Figure 1 | Proliferative activity and NGF and IL-1 $\beta$  secretion in Schwann cells and macrophages under different media.**  
Group A: Schwann cells in DMEM/F12; group B: Schwann cells in macrophage-conditioned medium; group C: Schwann cells in conditioned medium of macrophages activated by nerve homogenate; group D: Schwann cells in DMEM/F12 medium containing IL-1 $\beta$ ; group E: macrophages in DMEM/F12 medium; group F: macrophages in conditioned medium of macrophages activated by nerve homogenate; group G: macrophages in Schwann cell-conditioned medium; group H: macrophages in conditioned medium of Schwann cells activated by 2.0 ng/mL IL-1 $\beta$  medium. (A) The proliferation ability of Schwann cells cultured in different media was detected by EdU assay. Compared with the other three groups, group D had the largest number of EdU-positive cells, indicating that IL-1 $\beta$  had the strongest effect on Schwann cell proliferation. (B) The proliferation ability of macrophages cultured in different media was detected by EdU assay. There were more EdU-positive cells in groups F and H, indicating that conditioned medium of macrophages activated by nerve homogenate and conditioned medium of Schwann cells activated by IL-1 $\beta$  promoted macrophage proliferation. Scale bars: 100  $\mu$ m. (C) NGF expression in Schwann cells with different conditioned media by enzyme-linked immunosorbent assay. (D) IL-1 $\beta$  expression in macrophages with different conditioned media by enzyme-linked immunosorbent assay. Data are expressed as mean  $\pm$  SD. *In vitro* experiments were conducted three times independently. \*\* $P < 0.01$ , \*\*\* $P < 0.001$  (one-way analysis of variance followed by Student-Newman-Keuls *post hoc* test). DMEM/F12: Dulbecco's modified Eagle media: nutrient mixture F-12; IL: interleukin; NGF: nerve growth factor.

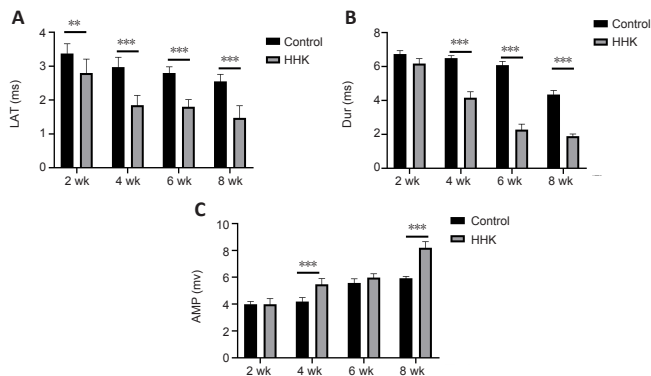


**Figure 2 | The bioactive artificial nerve improves nerve conduction capacity after sciatic nerve injury.**  
Control group: direct suture of sciatic nerve transection; HHK group: artificial nerve bridging was used after sciatic nerve transection. (A) The LAT index of the HHK group was significantly lower than that of the control group from 2 weeks. (B) The Dur index began to differ at 4 weeks. (C) At the 8<sup>th</sup> week, AMP in the HHK group was significantly higher than that in the control group. Data are expressed as mean  $\pm$  SD ( $n = 6$ ). \*\* $P < 0.01$ , \*\*\* $P < 0.001$  (independent sample *t*-test). Amp: Amplitude; Dur: duration; HHK: human hair keratin; LAT: latency.

**The bioactive artificial nerve affects the nerve repair factors in injured sciatic nerve**

Several important proteins related to nerve repair were detected by immunohistochemical staining. The numbers of FGF2- and TGFBR2-positive cells were significantly higher in the HHK group than those in the control group (Figure 6). The artificial nerve had no significant effect on the numbers of VEGF- and PDGFR- $\beta$ -positive cells. The results showed that the mechanism of promoting neural repair may be related to activation of the TGF signaling pathway and upregulation of FGF2 secretion.

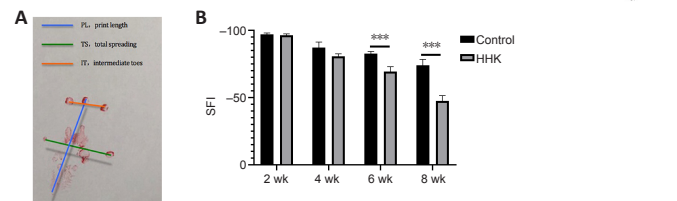


**Figure 3 | The bioactive artificial nerve improves sciatic function after sciatic nerve injury.**  
Control group: direct suture of sciatic nerve transection; HHK group: artificial nerve bridging was used after sciatic nerve transection. (A) Schematic diagram of the SFI measurement. (B) The sciatic nerve function index. Data are expressed as mean  $\pm$  SD ( $n = 6$ ). \*\*\* $P < 0.001$  (independent sample *t*-test). HHK: Human hair keratin; SFI: sciatic function index.

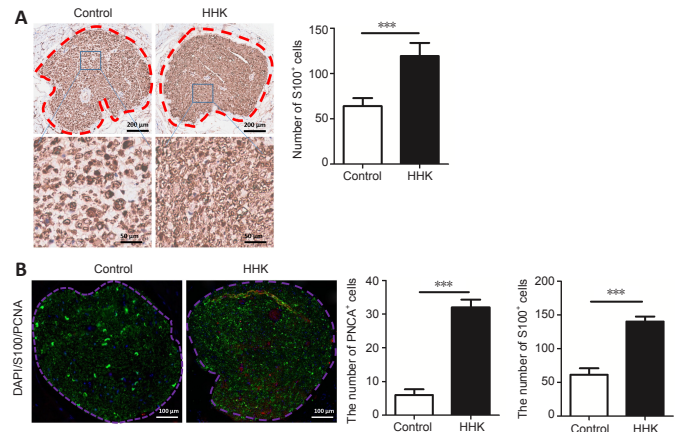


**Figure 4 | The bioactive artificial nerve promotes Schwann cell proliferation in the injured area after sciatic nerve injury.**  
Control group: direct suture of sciatic nerve transection; HHK group: artificial nerve bridging was used after sciatic nerve transection. (A) The number of S100-positive cells (green, stained by Dylight 488) was detected by immunohistochemical staining. The number of S100-positive cells in the control group was less than that in the HHK group. Scale bars: 200  $\mu$ m (upper), 50  $\mu$ m (lower). (B) Immunofluorescence staining was used for S100 (green, stained by Dylight 488) and PCNA (red, stained by Fluor594). The numbers of S100- and PCNA-positive cells in the control group were less than those in the HHK group. Scale bars: 100  $\mu$ m. Data are expressed as mean  $\pm$  SD ( $n = 6$ ). \*\*\* $P < 0.001$  (independent sample *t*-test). HHK: Human hair keratin; PCNA: proliferating cell nuclear antigen.

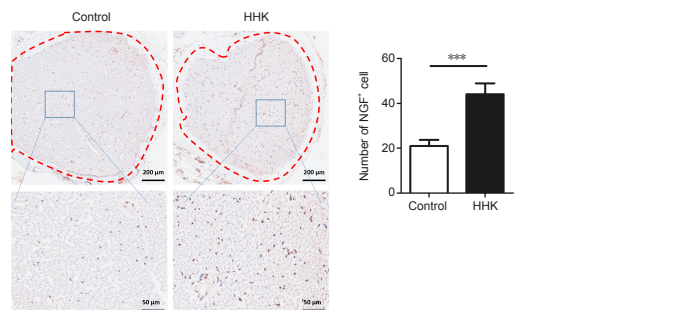


**Figure 5 | The bioactive artificial nerve promotes NGF secretion in sciatic nerve under *in situ* hybridization.**  
Control group: direct suture of sciatic nerve transection; HHK group: artificial nerve bridging was used after sciatic nerve transection. The number of NGF-positive cells in the HHK group was greater than that in the control group. Scale bars: 200  $\mu$ m (upper), 50  $\mu$ m (lower). Data are expressed as mean  $\pm$  SD ( $n = 6$ ). \*\*\* $P < 0.001$  (independent sample *t*-test). HHK: Human hair keratin; NGF: nerve growth factor.

**Discussion**

After peripheral nerve injury, Schwann cells induce macrophages and cytokines and regulate macrophage secretion of IL-1, which causes Schwann cells to secrete NGF. NGF is an insulin-like growth factor that promotes nutrition of TGF- $\beta$  and FGF2 secreted by macrophages, which in turn promote mitosis and Schwann cell proliferation (La Fleur et al., 1996; Cattin et al., 2015; Chen et al., 2015). Other studies have shown that IL-1 stimulates the continued expression of IL-1 in Schwann cells, and Schwann cells have

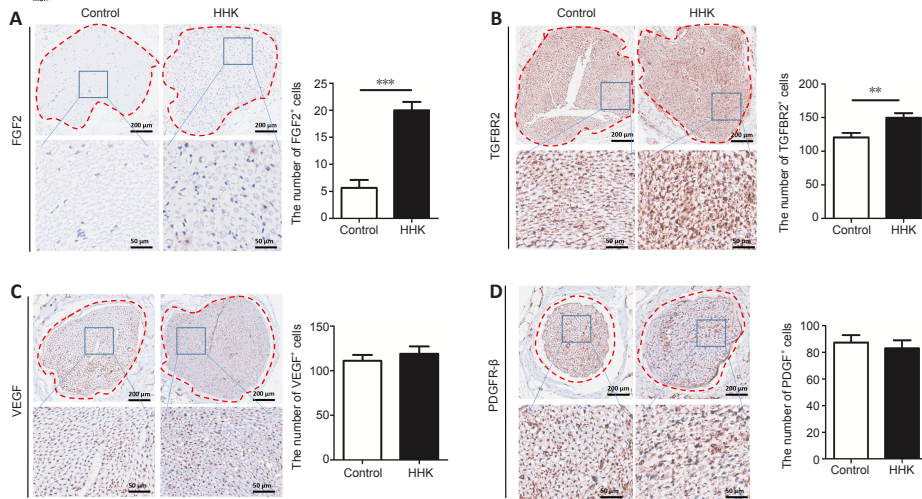


**Figure 6 | The bioactive artificial nerve affects nerve repair factors in injured sciatic nerve.**

Control group: direct suture of sciatic nerve transection; HHK group: artificial nerve bridging was used after sciatic nerve transection. (A–D) Numbers of FGF2-, TGFBR2-, VEGF- and PDGFR-β-positive cells. Scale bars: 200 μm (upper), 50 μm (lower). Data are expressed as mean ± SD (n = 6). \*\*P < 0.01, \*\*\*P < 0.001 (independent sample t-test). FGF2: Fibroblast growth factor-2; HHK: human hair keratin; PDGFR-β: platelet-derived growth factor receptor beta; TGFBR2: transforming growth factor beta receptor type 2; VEGF: vascular endothelial growth factor.

autocrine and paracrine regulation of IL-1. In the inflammatory state, IL-1 expression activates cytokine signals at nerve injury sites and changes pathological conditions by secreting cytokines. In addition, IL-1 functions differently from other inflammatory factors, such as TNF-α, which induces Schwann cell demyelination, and IFN-γ, which induces Schwann cell apoptosis. IL-1 mainly induces Schwann cell proliferation and has antigen-presenting functions, and is an important factor in initiating immune response and nerve repair (Lisak et al., 1994; Skundric et al., 1997; Créange et al., 1998; Conti et al., 2002; Ozaki et al., 2008). High expression of IL-1β may help fibroblasts secrete granulocyte macrophage colony-stimulating factor and induce Schwann cells to secrete NGF and promote nerve regeneration (Chen et al., 2015). Although IL-1β and NGF overexpression has been reported to cause neuropathic pain (Dai et al., 2020; Khan et al., 2021), we did not find any significant pain differences between the two groups after surgery, suggesting that the new artificial nerve transplantation did not bring obvious pain to the rats. However, more detailed pain tests are needed to confirm this conclusion.

Sierpinski et al. (Sierpinski et al., 2008) bridged a 4-mm tibial nerve defect in mice using an HHK nerve catheter and induced nerve fibers to regenerate under tension-free conditions. They reported that HHK significantly improved nerve function by bridging neural dendritic restoration through nerve conduction pathways while regeneration of degradation products induced Schwann cells and nerve fibers (Sierpinski et al., 2008). In this study, neural bridges constructed by coculture of Schwann cells activated by HHK and IL-1β were used to repair nerve defects. By providing adhesive media, space and direction for Schwann cells, the longitudinal HHK microfilament structure promoted Schwann cell growth and nerve fiber regeneration. Our experimental results showed that the number of Schwann cells in the HHK group was significantly higher and the proliferation rate was faster, which facilitated nerve repair.

To further verify this finding and determine whether the constructed artificial nerve promotes nerve functional recovery, we evaluated peripheral nerve function by SFI index and electrophysiology. In addition to indicating muscle strength recovery at the lower extremities, SFI also assesses muscle coordination function and can be dynamically observed. SFI is reliable and accurate in evaluation of sciatic nerve functional recovery. Motor nerve conduction velocity reflects not only nerve stem conduction function but also neuromuscular junction function. Conduction velocity recovery and amplitude changes in early and late stages also indicate myelin regeneration in demyelinated peripheral nerves (Valentino et al., 2007). In this study, the results of neuroelectrophysiology and SFI indexes showed that all measures of the constructed artificial nerve after transplantation were significantly improved compared with those in the control group, suggesting that the artificial nerve bridging led to better neural regeneration and repair function than the direct suture technique.

Many studies have shown that FGF2, TGFBR2, VEGF and PDGFR2 also play important roles in nerve repair. FGF2, also known as basic FGF, is a multi-functional growth factor. High expression of FGF2, one of the 22-member FGF family, can be detected upon the onset of neurodevelopment (Murphy et al., 1994). Consistent with its role in neurogenesis and synaptic enhancement, FGF2 has been shown to be highly effective in neuronal regeneration in a variety of experimental animal models, including models of optic nerve injury and excitatory toxic cell death, as well as in the treatment of neurodegenerative diseases such as Alzheimer's disease and Parkinson's disease (Sapieha et al., 2003; Kiyota et al., 2011). Similarly, TGFBR2 has been found to be effective in preventing neurodegeneration and maintaining normal nerve function (Tesseur et al., 2006). Interestingly, FGF2 and TGF have been reported to coregulate neuronal survival (Kriegstein et al., 1998). In our study, we found that the expression of FGF2 and TGFBR2 was upregulated in the HHK group compared with that in the control group, suggesting that the constructed artificial nerve may promote the repair of damaged nerves by upregulating FGF2 and TGF-β signaling pathways. Nerve function repair is closely related to blood vessels, and VEGF plays a crucial role in blood vessel

formation. Pan et al.'s study (Pan et al., 2013) has shown that VEGF promotes peripheral nerve repair. The PDGF signaling pathway not only promotes the neurite induction activity of Schwann cells and activates Schwann cells (Sowa et al., 2019), but also affects the role of endothelial progenitor cells in promoting nerve repair (Fang et al., 2020). However, there were no significant differences in VEGF or PDGFR-β expression between the HHK group and the control group in our study. Together, these results suggest that the constructed artificial nerve promoted secretion of NGF, FGF2 and other important nerve factors, but had a weak effect on repair of vessels and other auxiliary nerves.

In summary, the HHK artificial nerve-bridge graft accelerated nerve repair by providing better spatial structure for nerve regeneration, and promoting proliferation of Schwann cells and secretion of neural factors such as NGF. A possible mechanism for the enhanced neural repair is activation of FGF2 and TGF-β signaling pathways. Our paper has some limitations. For example, we did not investigate the effect of different IL-1β concentrations for Schwann cell activation on the HHK artificial nerve and whether there was an optimal IL-1β concentration. In addition, we selected only some neural repair factors for detection, which were not comprehensive. Further transcriptomic or proteomic sequencing would provide more comprehensive information on HHK artificial peripheral nerve repair and provide further insight for signal mechanism studies. In conclusion, the findings indicate that compared with direct simple nerve suture, compound culture of IL-1β-activated Schwann cells and HHK to construct an artificial nerve graft may be advantageous for the repair of sciatic nerve defects. The newly constructed artificial nerve has good biological properties, which can not only be used to repair a large area of nerve defects, but also better promote the repair of nerve function. It is a relatively ideal nerve graft. In addition, the study also showed that artificial nerve construction with high biological activity may be a feasible and effective approach for nerve repair. Our study provides a new perspective for the study of nerve grafts.

**Author contributions:** Study conception and design: JY, BY; experiment implementation: JY, HJQ; data analysis: JZC, KRZ, JQQ, XQZ; manuscript draft: HJQ, HL. All authors reviewed and approved the final version of the manuscript.

**Conflicts of interest:** The authors have declared that no competing interests exist.

**Availability of data and materials:** All data generated or analyzed during this study are included in this published article and its supplementary information files.

**Open access statement:** This is an open access journal, and articles are distributed under the terms of the Creative Commons AttributionNonCommercial-ShareAlike 4.0 License, which allows others to remix, tweak, and build upon the work non-commercially, as long as appropriate credit is given and the new creations are licensed under the identical terms.

**Additional files:**

**Additional Figure 1:** The flowchart of the study.

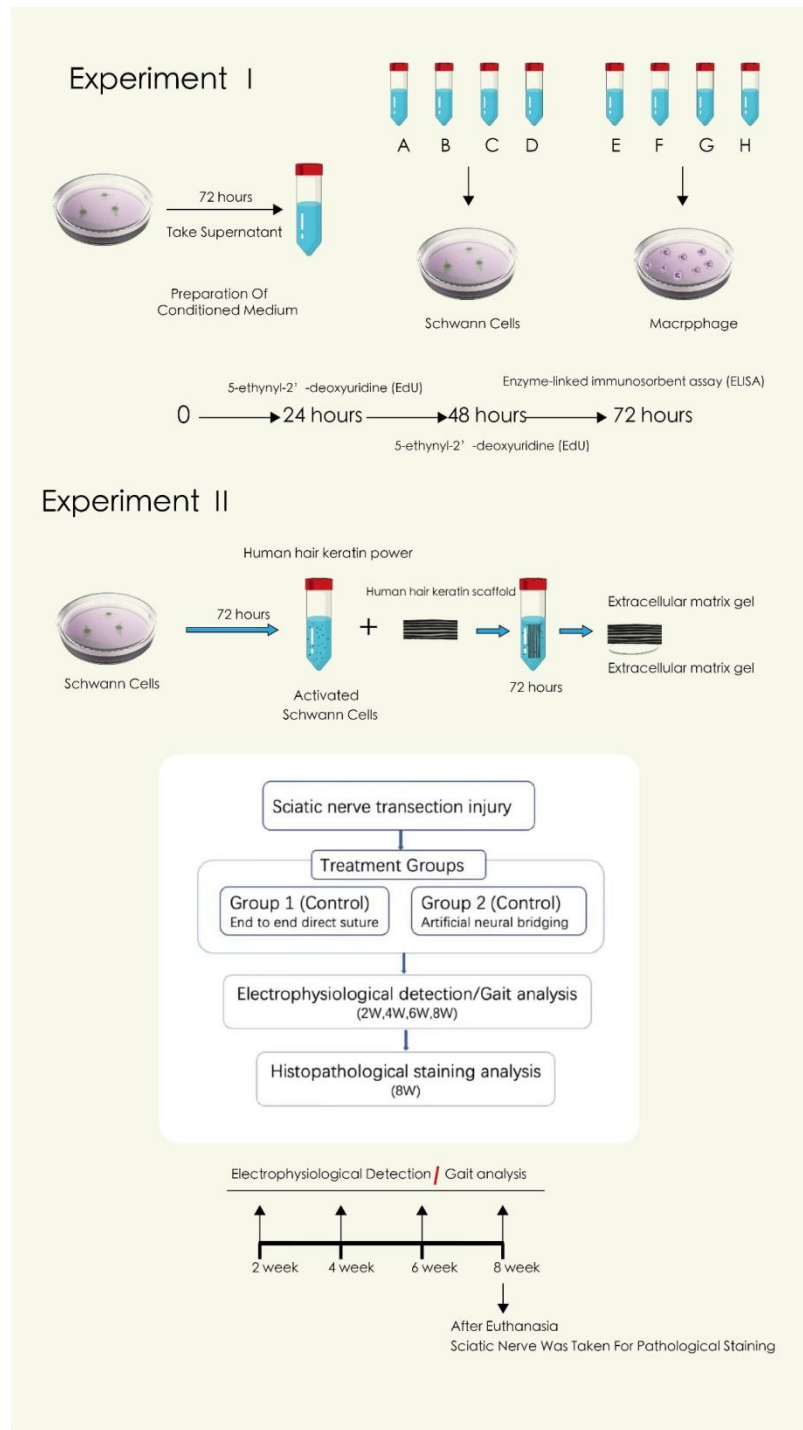
**Additional Figure 2:** Electron microscopic observation of HHK artificial nerve.

## References

- Benowitz LI, Popovich PG (2011) Inflammation and axon regeneration. *Curr Opin Neurol* 24:577-583.
- Campbell WW (2008) Evaluation and management of peripheral nerve injury. *Clin Neurophysiol* 119:1951-1965.

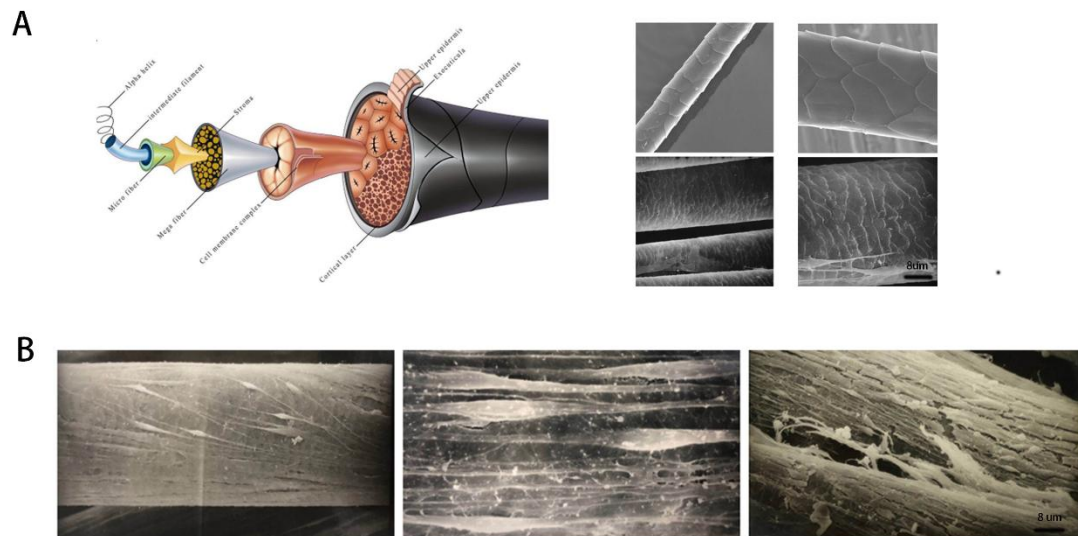
- Cattin AL, Lloyd AC (2016) The multicellular complexity of peripheral nerve regeneration. *Curr Opin Neurobiol* 39:38-46.
- Cattin AL, Burden JJ, Van Emmenis L, Mackenzie FE, Hoving JJ, Garcia Calavia N, Guo Y, McLaughlin M, Rosenberg LH, Quereda V, Jamecna D, Napoli I, Parrinello S, Enver T, Ruhrberg C, Lloyd AC (2015) Macrophage-induced blood vessels guide schwann cell-mediated regeneration of peripheral nerves. *Cell* 162:1127-1139.
- Chen P, Piao X, Bonaldo P (2015) Role of macrophages in Wallerian degeneration and axonal regeneration after peripheral nerve injury. *Acta Neuropathol* 130:605-618.
- Chiono V, Tonda-Turo C (2015) Trends in the design of nerve guidance channels in peripheral nerve tissue engineering. *Prog Neurobiol* 131:87-104.
- Clements MP, Byrne E, Camarillo Guerrero LF, Cattin AL, Zakka L, Ashraf A, Burden JJ, Khadayat S, Lloyd AC, Marguerat S, Parrinello S (2017) The wound microenvironment reprograms schwann cells to invasive mesenchymal-like cells to drive peripheral nerve regeneration. *Neuron* 96:98-114.e7.
- Conti G, De Pol A, Scarpini E, Vaccina F, De Riz M, Baron P, Tiriticco M, Scarlato G (2002) Interleukin-1 beta and interferon-gamma induce proliferation and apoptosis in cultured Schwann cells. *J Neuroimmunol* 124:29-35.
- Créange A, Lefaucheur JP, Authier FJ, Gherardi RK (1998) Cytokines and peripheral neuropathies. *Rev Neurol (Paris)* 154:208-216.
- Dai WL, Yan B, Bao YN, Fan JF, Liu JH (2020) Suppression of peripheral NGF attenuates neuropathic pain induced by chronic constriction injury through the TAK1-MAPK/NF- $\kappa$ B signaling pathways. *Cell Commun Signal* 18:66.
- de Guzman RC, Merrill MR, Richter JR, Hamzi RI, Greengauz-Roberts OK, Van Dyke ME (2011) Mechanical and biological properties of keratose biomaterials. *Biomaterials* 32:8205-8217.
- Fang J, Huang X, Han X, Zheng Z, Hu C, Chen T, Yang X, Ouyang X, Chen Z, Wei H (2020) Endothelial progenitor cells promote viability and nerve regenerative ability of mesenchymal stem cells through PDGF-BB/PDGFR- $\beta$  signaling. *Aging (Albany NY)* 12:106-121.
- Gu X, Ding F, Williams DF (2014) Neural tissue engineering options for peripheral nerve regeneration. *Biomaterials* 35:6143-6156.
- Gu X, Ding F, Yang Y, Liu J (2011) Construction of tissue engineered nerve grafts and their application in peripheral nerve regeneration. *Prog Neurobiol* 93:204-230.
- Hu TT, Chang SS, Wei ZR (2022) Macrophage polarization effectively promotes nerve regeneration after peripheral nerve injury through the M2 phenotypic regulation. *Zhongguo Zuzhi Gongcheng Yanjiu* 26:2285-2290.
- Hwang JY, Shin US, Jang WC, Hyun JK, Wall IB, Kim HW (2013) Biofunctionalized carbon nanotubes in neural regeneration: a mini-review. *Nanoscale* 5:487-497.
- Jessen KR, Mirsky R (2016) The repair Schwann cell and its function in regenerating nerves. *J Physiol* 594:3521-3531.
- Kessler CM, Benchikh El Fegoun S, Worster A (2018) Methodologies for data collection in congenital haemophilia with inhibitors (CHwi): critical assessment of the literature and lessons learned from recombinant factor VIIa. *Haemophilia* 24:536-547.
- Khan J, Wang Q, Ren Y, Eliav R, Korczeniewska OA, Benoliel R, Eliav E (2021) Exercise induced hypoalgesia profile in rats is associated with IL-10 and IL-1  $\beta$  levels and pain severity following nerve injury. *Cytokine* 143:155540.
- Kiani MT, Higgins CA, Almquist BD (2018) The hair follicle: an underutilized source of cells and materials for regenerative medicine. *ACS Biomater Sci Eng* 4:1193-1207.
- Kilkenny C, Browne WJ, Cuthill IC, Emerson M, Altman DG (2010) Improving bioscience research reporting: the ARRIVE guidelines for reporting animal research. *PLoS Biol* 8:e1000412.
- Kiyota T, Ingraham KL, Jacobsen MT, Xiong H, Ikezu T (2011) FGF2 gene transfer restores hippocampal functions in mouse models of Alzheimer's disease and has therapeutic implications for neurocognitive disorders. *Proc Natl Acad Sci U S A* 108:E1339-1348.
- Knowlton S, Anand S, Shah T, Tasoglu S (2018) Bioprinting for neural tissue engineering. *Trends Neurosci* 41:31-46.
- Kriegelstein K, Farkas L, Unsicker K (1998) TGF- $\beta$  regulates the survival of ciliary ganglionic neurons synergistically with ciliary neurotrophic factor and neurotrophins. *J Neurobiol* 37:563-572.
- La Fleur M, Underwood JL, Rappolee DA, Werb Z (1996) Basement membrane and repair of injury to peripheral nerve: defining a potential role for macrophages, matrix metalloproteinases, and tissue inhibitor of metalloproteinases-1. *J Exp Med* 184:2311-2326.
- Li C, Liu SY, Pi W, Zhang PX (2021) Cortical plasticity and nerve regeneration after peripheral nerve injury. *Neural Regen Res* 16:1518-1523.
- Lisak RP, Bealmear B, Ragheb S (1994) Interleukin-1 alpha, but not interleukin-1 beta, is a co-mitogen for neonatal rat Schwann cells in vitro and acts via interleukin-1 receptors. *J Neuroimmunol* 55:171-177.
- Liu Y, Dai X, Yang S, Peng Y, Hou F, Zhou Q (2021) High salt aggravates renal inflammation via promoting pro-inflammatory macrophage in 5/6-nephrectomized rat. *Life Sci* 274:119109.
- Murphy M, Reid K, Ford M, Furness JB, Bartlett PF (1994) FGF2 regulates proliferation of neural crest cells, with subsequent neuronal differentiation regulated by LIF or related factors. *Development* 120:3519-3528.
- Ozaki A, Nagai A, Lee YB, Myong NH, Kim SU (2008) Expression of cytokines and cytokine receptors in human Schwann cells. *Neuroreport* 19:31-35.
- Pace LA, Plate JF, Smith TL, Van Dyke ME (2013) The effect of human hair keratin hydrogel on early cellular response to sciatic nerve injury in a rat model. *Biomaterials* 34:5907-5914.
- Pan Z, Fukuoka S, Karagianni N, Guaiquil VH, Rosenblatt MI (2013) Vascular endothelial growth factor promotes anatomical and functional recovery of injured peripheral nerves in the avascular cornea. *FASEB J* 27:2756-2767.
- Rao F, Wang Y, Zhang D, Lu C, Cao Z, Sui J, Wu M, Zhang Y, Pi W, Wang B, Kou Y, Wang X, Zhang P, Jiang B (2020) Aligned chitosan nanofiber hydrogel grafted with peptides mimicking bioactive brain-derived neurotrophic factor and vascular endothelial growth factor repair long-distance sciatic nerve defects in rats. *Theranostics* 10:1590-1603.
- Sapieha PS, Peltier M, Rendahl KG, Manning WC, Di Polo A (2003) Fibroblast growth factor-2 gene delivery stimulates axon growth by adult retinal ganglion cells after acute optic nerve injury. *Mol Cell Neurosci* 24:656-672.
- Schultz JD, Dodson TB, Meyer RA (1992) Donor site morbidity of greater auricular nerve graft harvesting. *J Oral Maxillofac Surg* 50:803-805.
- Shavandi A, Silva TH, Bekhit AA, Bekhit AEA (2017) Keratin: dissolution, extraction and biomedical application. *Biomater Sci* 5:1699-1735.
- Sierpinski P, Garrett J, Ma J, Apel P, Klorig D, Smith T, Koman LA, Atala A, Van Dyke M (2008) The use of keratin biomaterials derived from human hair for the promotion of rapid regeneration of peripheral nerves. *Biomaterials* 29:118-128.
- Skundric DS, Bealmear B, Lisak RP (1997) Induced upregulation of IL-1, IL-1RA and IL-1R type I gene expression by Schwann cells. *J Neuroimmunol* 74:9-18.
- Sowa Y, Kishida T, Tomita K, Adachi T, Numajiri T, Mazda O (2019) Involvement of PDGF-BB and IGF-1 in activation of human schwann cells by platelet-rich plasma. *Plast Reconstr Surg* 144:1025e-1036e.
- Tao Y (2013) Isolation and culture of Schwann cells. *Methods Mol Biol* 1018:93-104.
- Tesseur I, Zou K, Esposito L, Bard F, Berber E, Can JV, Lin AH, Crews L, Tremblay P, Mathews P, Mucke L, Masliah E, Wyss-Coray T (2006) Deficiency in neuronal TGF- $\beta$  signaling promotes neurodegeneration and Alzheimer's pathology. *J Clin Invest* 116:3060-3069.
- Valentino DJ, Walter RJ, Dennis AJ, Nagy K, Looor MM, Winners J, Bokhari F, Wiley D, Merchant A, Joseph K, Roberts R (2007) Neuromuscular effects of stun device discharges. *J Surg Res* 143:78-87.
- Wang GW, Yang H, Wu WF, Zhang P, Wang JY (2017) Design and optimization of a biodegradable porous zein conduit using microtubes as a guide for rat sciatic nerve defect repair. *Biomaterials* 131:145-159.
- Xu XJ, Piao YJ, Huo X (2003) Effect of human hair keratin implant on oligodendrocyte proliferation and differentiation in rats with acute spinal cord injury. *Di Yi Jun Yi Da Xue Xue Bao* 23:542-545.

C-Editor: Zhao M; S-Editors: Yu J, Li CH; L-Editors: McCollum L, Song LP; T-Editor: Jia Y



**Additional Figure 1 The flow chart of the study.**

Group A: Schwann cells in DMEM/F12; group B: Schwann cells in macrophage conditioned medium; group C: Schwann cells in conditioned medium of macrophages activated by nerve homogenate; group D: Schwann cells in DMEM/F12 medium containing IL-1 $\beta$ ; group E: macrophages in DMEM/F12 medium; group F: macrophages in conditioned medium of macrophages activated by nerve homogenate; group G: macrophages in Schwann cell conditioned medium; group H: macrophages in conditioned medium of Schwann cells activated by 2.0 ng/mL IL-1 $\beta$  medium. DMEM/F12: Dulbecco's modified Eagle media: nutrient mixture F-12; IL: interleukin.



**Additional Figure 2 Electron microscopic observation of HHK artificial nerve**

(A) Schematic diagram of human hair composition and electron microscope view of HHK scaffold. (B) HHK artificial neural electron microscope image after successful construction. Scale bars: 8 μm.